

# Prelaunch Characteristics of the Moderate Resolution Imaging Spectroradiometer (MODIS) on EOS-AM1

William L. Barnes, Thomas S. Pagano, and Vincent V. Salomonson, *Fellow, IEEE*

**Abstract**—The Moderate Resolution Imaging Spectroradiometer (MODIS), with 36 bands and 0.25-, 0.5-, and 1.0-km geometric instantaneous-fields-of-view (GIFOV's) at nadir, has completed system level testing and has been integrated onto the Earth Observing System (EOS)-AM1 spacecraft, which is slated for launch in 1998.

Raytheon Santa Barbara Remote Sensing (SBRS), Goleta, CA, the MODIS developer, has performed extensive characterization and calibration measurements that have demonstrated a system that meets or exceeds most of NASA's demanding requirements. Based on this demonstrated capability, the MODIS Science Team, an international group of 28 land, ocean, atmosphere, and calibration remote-sensing scientists, has commenced delivery of algorithms that will routinely calculate 42 MODIS standard data products postlaunch. These products range from atmospheric aerosols, snow cover, and land and water surface temperature to leaf area index, ocean chlorophyll concentration, and sea ice extent, to name just a few. A description of the Science Team, including members' research interests and descriptions of their MODIS algorithms, can be found at the MODIS homepage (<http://ltpwww.gsfc.nasa.gov/MODIS/MODIS.html>).

The MODIS system level testing included sufficient measurements in both ambient and thermal-vacuum environments to both demonstrate specification compliance and enable postlaunch implementation of radiometric calibration algorithms. The latter will include calculations to account for changes in response versus scan angle, response versus temperature, and response linearity. The system level tests also included performance verification of the onboard calibration systems, including the solar diffuser stability monitor (SDSM), the blackbody (BB), and the spectral radiometric calibration assembly (SRCA), which will enable monitoring of MODIS performance postlaunch. Descriptions of these subsystems are also on the MODIS homepage.

**Index Terms**—Calibration, image sensors, optical spectroscopy, radiometry, remote sensing, space technology.

## I. BACKGROUND

THE MODERATE Resolution Imaging Spectroradiometer (MODIS) is a major instrument on the Earth Observing System (EOS)-AM1 and EOS-PM1 missions [1]. The MODIS has the capability to observe nearly the entire earth every two days via a set of 36 spectral bands at nadir geometric instantaneous-fields-of-view (GIFOV's) of 250, 500, and 1000 m and provide key observations important to studies

of the atmosphere, oceans, and land surfaces. The "heritage" of the MODIS comes from several spaceborne instruments. These include the Advanced Very High Resolution Radiometer (AVHRR) and the High Resolution Infrared Sounder (HIRS) unit on the National Oceanic and Atmospheric Administration's (NOAA) Polar Orbiting Operational Environmental Satellites (POES), the Nimbus-7 Coastal Zone Color Scanner (CZCS), and the Landsat Thematic Mapper (TM). The MODIS will be able to continue and extend the databases acquired over many years by the AVHRR, in particular, and the CZCS/SeaStar-SeaWiFS series. The MODIS will also measure new data sets that are important to studies of the earth as a total system, with emphasis on interactions between the atmosphere, land, and oceans.

The MODIS was originally conceived as a system composed of two instruments called MODIS-N (nadir) and MODIS-T (tilt), which were slated for flight on the EOS-AM platforms. These two instruments were described in various levels of detail in studies as far back as 1985 [2]–[4]. MODIS-T was designed basically as an advanced ocean color sensor with the ability to tilt to avoid sunglint [6]. The MODIS-T instrument was eventually removed from further development as the budget for EOS became more constrained. In order to minimize the impact of the loss of MODIS-T and meet or approach other scientific objectives that were not being met up to that time, such as observations of the diurnal variation in the earth's cloudiness, MODIS-N was also placed on the EOS-PM platforms. This enabled morning and afternoon observations to be obtained. The two MODIS instruments could, in combination, obtain more ocean color coverage than one (e.g., one MODIS on the EOS-AM1 mission) could (i.e., reduce data loss due to sunglint), but not as much as MODIS-N and MODIS-T on one platform. The overall cost was reduced because the MODIS-N and a copy (recurring cost only) would be less than MODIS-N and T together (two nonrecurring costs).

As the result of the loss of MODIS-T, the MODIS-N was simply called the MODIS. However, between 1989 and the present, the original concept for MODIS-N experienced several changes, including the number and placement of bands for the instrument. The 40-band instrument envisioned in 1989 was reduced to a 36-band instrument so as to reduce estimated cost and complexity. Within the 36 bands on the MODIS, there are three major band segments (see Table II). There are seven bands (bands numbered 1–7 in Table II) that will observe land cover features plus cloud and aerosol properties [7]–[9]. The spectral placement of these bands are derived so as to be very similar to the bands on the Landsat TM, albeit the

Manuscript received November 11, 1997; revised February 19, 1998 and March 16, 1998.

W. L. Barnes and V. V. Salomonson are with the Earth Sciences Directorate, NASA's Goddard Space Flight Center, Greenbelt, MD 20771 USA (e-mail: [wbarne@neptune.gsfc.nasa.gov](mailto:wbarne@neptune.gsfc.nasa.gov); [vsalomon@pop900.gsfc.nasa.gov](mailto:vsalomon@pop900.gsfc.nasa.gov)).

T. S. Pagano was with Raytheon Santa Barbara Remote Sensing, Goleta, CA 93117 USA. He is now with the Jet Propulsion Laboratory, California Institute of Technology, Pasadena, CA 91109 USA.

Publisher Item Identifier S 0196-2892(98)04807-4.

TABLE I  
NASA PERFORMANCE REQUIREMENTS AND SBRS DESIGN CHOICES

Orbit	705 km, 10:30 a.m. descending node or 1:30 p.m. ascending node, sun-synchronous, near-polar, circular
Swath Width	2330 km (cross track)
*Swath Length	10 km (along track at nadir)
*Scan Rate	20.3 rpm, cross track
*Telescope	17.78 cm diam. off-axis, afocal (collimated), with intermediate field stop
Size	1.0 x 1.6 x 1.0 m
Weight	250 kg
Power	225 W (orbital average)
Spectral Bands	36 (See Table 2.)
Spatial Resolution	250 m (bands 1-2) 500 m (bands 3-7) 1000 m (bands 8-36)
*Data Rate	11 Mbps (peak daytime)
*Quantization	12 bits
Design Life	5 years

spatial resolutions are 250 or 500 m, depending on the MODIS band involved. There are nine ocean color bands (bands 8–16) that were derived from the studies leading to the Nimbus CZCS and the SeaWiFS instrument [10], [11]. Another set of bands (bands 20–25 and 27–36) were drawn from the bands of the HIRS, with emphasis on those HIRS bands that sense properties of the troposphere and the surface [12].

In the original concept for the MODIS-N, there were three bands near 700 nm that were to measure polarization that were dropped along with three bands near 760 nm that would observe optical properties of clouds in the oxygen-A band absorption region. These were replaced by one broad and two narrow bands near 900 nm (bands 17–19 in Table II) that were derived from analyses of data from the airborne AVIRIS instrument. These bands enable water-vapor observations in the lower troposphere as well as some cloud properties that were deemed advantageous [8], [13], [14]. There was a need to make further reductions in the predicted overall cost of the MODIS so two separate 250-m spatial resolution bands at 575 and 880 nm were combined with two 500-m bands at roughly the same center wavelengths. This resulted in a compromise (bands 1 and 2), whereby the 250-m spatial resolution was retained but with 50- and 35-nm bandwidths that were somewhat broader than the bandwidths associated with the original 500-m bands. Finally, more analyses of the AVIRIS data indicated high value in gathering cirrus cloud observations by adding a band at 1.38  $\mu\text{m}$  [15], [16]. To keep the number of MODIS bands limited to no more than 36, it was decided to replace a 3.959- $\mu\text{m}$  atmospheric sounding band (band 26) with the 1.38- $\mu\text{m}$  capability.

## II. REQUIREMENTS AND DESIGN TRADEOFFS

Based on inputs generated by an *ad hoc* science team [3] and the results from system design studies [4], [5], a set of performance specifications [17] were generated by personnel at NASA's Goddard Space Flight Center (GSFC), Greenbelt, MD, in 1990. These were subsequently used in the selection of Raytheon Santa Barbara Remote Sensing (SBRS), Goleta, CA, as the MODIS development contractor. A top-level synopsis of these requirements is given in Tables I and II. Table I also

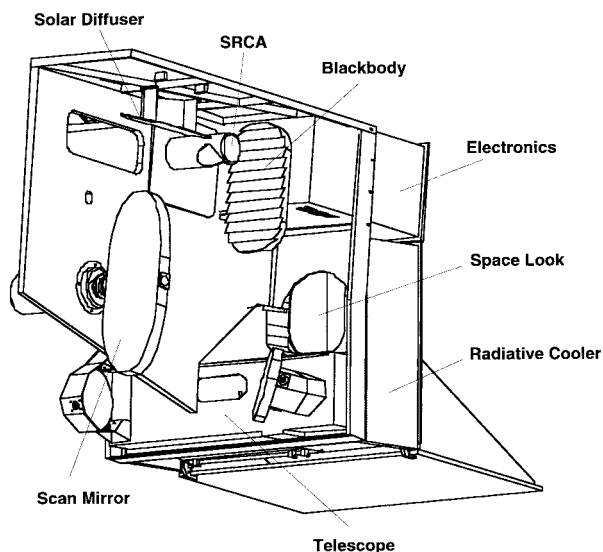


Fig. 1. MODIS subsystems.

contains several design choices (\*) made by SBRS in meeting these requirements. A few of the major system tradeoffs are outlined below to illustrate the origins of the MODIS design.

Image generation from low earth orbit is generally limited to either cross-track scanning with a rotating mirror that successively views pixels across a swath on the earth's surface or a pushbroom approach wherein long linear arrays of detectors view across the swath. In both cases, the orbital motion of the spacecraft generates the second dimension of the image. Due to the number of bands and the 2330-km swath, a pushbroom system was considered impractical and cross-track scanning was chosen for the MODIS design. There are several choices to be made in implementing a cross-track scanner, including the number of along-track detectors in each spectral band, which determines the number of lines viewed during each scan across the swath and scan mirror geometry. These, together with tradeoffs in required sensitivity, optics size, band-to-band registration, and scan rates, led the MODIS designers to a double-sided, continuous rotation, paddle wheel scan mirror (see Fig. 1) and a 10-km

TABLE II  
MODIS SPECTRAL BANDS

Primary Use	Band No.	Bandwidth (nm)	Spectral Radiance	Required SNR
Land/Cloud Boundaries	1**	620-670	21.8	128
	2**	841-876	24.7	201
Land/Cloud Properties	3*	459-479	35.3	243
	4*	545-565	29.0	228
	5*	1230-1250	5.4	74
	6*	1628-1652	7.3	275
	7*	2105-2155	1.0	110
Ocean Color/ Phytoplankton/ Biogeochemistry	8	405-420	44.9	880
	9	438-448	41.9	838
	10	483-493	32.1	802
	11	526-536	27.9	754
	12	546-556	21.0	750
	13	662-672	9.5	910
	14	673-683	8.7	1087
	15	743-753	10.2	586
Atmospheric Water Vapor	16	862-877	6.2	516
	17	890-920	10.0	167
	18	931-941	3.6	57
	19	915-965	15.0	250

\* 500m Spatial Resolution

\*\* 250m Spatial Resolution

Spectral Radiance values are in  $W/m^2\text{-}\mu\text{m-sr}$

SNR = Signal-to-noise ratio

(a)

Primary Use	Band	Bandwidth ( $\mu\text{m}$ )	Spectral Radiance	Required NEDT (K)
Surface/Cloud Temperature	20	3.660-3.840	0.45(300K)	0.05
	21	3.929-3.989	2.38(335K)	2.00
	22	3.929-3.989	0.67(300K)	0.07
	23	4.020-4.080	0.79(300K)	0.07
Atmospheric Temperature	24	4.433-4.498	0.17(250K)	0.25
	25	4.482-4.549	0.59(275K)	0.25
Cirrus Clouds Water Vapor	26	1.360-1.390	6.00	150 (SNR)
	27	6.535-6.895	1.16(240K)	0.25
	28	7.175-7.475	2.18(250K)	0.25
	29	8.400-8.700	9.58(300K)	0.05
Ozone	30	9.580-9.880	3.69(250K)	0.25
Surface/Cloud Temperature	31	10.780-11.280	9.55(300K)	0.05
	32	11.770-12.270	8.94(300K)	0.05
Cloud Top Altitude	33	13.185-13.485	4.52(260K)	0.25
	34	13.485-13.785	3.76(250K)	0.25
	35	13.785-14.085	3.11(240K)	0.25
	36	14.085-14.385	2.08(220K)	0.35

Spectral Radiance values are in  $W/m^2\text{-}\mu\text{m-sr}$

NEDT = Noise-equivalent temperature difference

(b)

along-track field-of-view (FOV). Thus, each 1-km band has a ten-element linear detector array with a spectral interference filter in close proximity and each of the 250-m and 500-m bands have 40 and 20 element arrays, respectively.

The required MODIS sensitivities (SNR's and NEDT's), spatial resolutions, swath width, and orbital altitude, together with spectral bandwidths, detector responses, and the scan-

ning approach discussed above, dictate an optical aperture of approximately 18-cm diameter. This diameter, together with the swath width requirement, results in a scan mirror length of 60 cm, which in turn, governs the overall size of MODIS.

Early in the design phase, consideration was given to hyperspectral approaches (spectrometers or interferometers) for spectral band definition. But, due to the large differences in

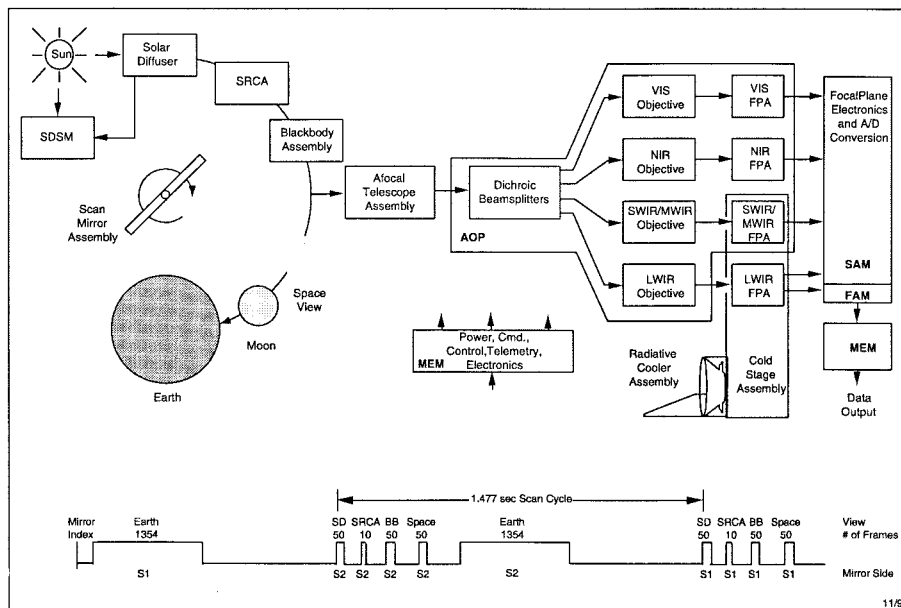


Fig. 2. MODIS functional design.

dynamic range between bands, spectral overlap of numerous bands, and the requirement for several spatial resolutions, this was deemed impractical and interference filters were chosen for spectral delineation.

The remaining top-level trade is the aft optics approach. Since 16 of the MODIS bands require cryogenic cooling of their detector arrays, at least two focal planes are required (i.e., cooled and uncooled). However, focal planes with 16-20 bands each are very complex, result in wide cross-track FOV's (and consequent scattered light problems) and complicate band-to-band registration. Therefore, the decision was made to use four focal planes in the MODIS design, including visible (VIS), near infrared (NIR), shortwave and midwave infrared (SW/MWIR), and longwave infrared (LWIR) focal planes. The spectral radiance impinging on each of these is delineated via three dichroic beam splitters. The SW/MWIR and LWIR focal plane assemblies (FPA's) are cooled to approximately 85 K by a passive radiative cooler.

There are innumerable trades that must be made in arriving at a final design for a complex remote-sensing system. The preceding discussion attempts to outline how the system requirements and current technology readiness governed some of the major MODIS design decisions.

### III. SYSTEM DESIGN

A schematic of the MODIS design is shown in Fig. 2. Each side of the scan mirror successively views a series of onboard calibration devices and 1354 earth view pixels across the  $\pm 55^\circ$  swath in 1.477 s (see bottom of Fig. 2). The energy reflected off the scan mirror is collected by an afocal telescope, divided spectrally by the three beam splitters mentioned above, and then transmitted through four refractive objectives onto the four FPA's. Output signals from the FPA's are digitized to 12-bit precision, processed, packetized, and sent to the spacecraft for storage and/or transmittal to the ground.

#### A. Optics

The double-sided beryllium scan mirror is  $57.8 \times 21.0 \times 5.0$  cm, has been lightweighted to 4.3 kg, and requires only 1 W to maintain its operational speed of 20.3 rpm. Mirror position is monitored via a 14-bit optical encoder, and the optical surfaces are nickel plated, polished, coated with silver, and overcoated with a protective layer. Due to the variation of emissivity with scan angle (see Section IV), the temperature of the mirror must be known to better than 1.0 K for calibration purposes. Therefore, a noncontact thermistor probe is inserted along the mirror rotation axis on the side opposite the motor mount.

The scan mirror passes energy onto a fold mirror (see Fig. 1) and then to the primary of an afocal Gregorian telescope consisting of two off-axis confocal parabolic mirrors. An intermediate field stop between the two mirrors is used to limit stray light passing to the aft optics. The fold mirror and telescope are kinematically mounted on a graphite epoxy optical bench.

A second graphite epoxy structure, the aft optics platform, serves as the optical bench for the dichroic beam splitter assembly and the four objective assemblies. Also mounted to this structure are the telescope assembly and the passive radiative cooler. The two cooled FPA's are mounted on the cold patch of the cooler and the VIS and NIR FPA's are mounted to their objectives.

#### B. Focal Plane Assemblies

The four MODIS FPA's consist of detector arrays, readout integrated circuits (ROIC's), and a filter bezel with bandpass and blocking filters for 7-10 bands. Each detector element has numerous indium bumps that are mated to similar bumps on the ROIC's leading to individual preamplifiers. Detector elements range from 135- to 540- $\mu\text{m}$  square.

As mentioned in the previous section, the 1000-m bands have ten detector elements each, the 500-m bands have 20, and the 250-m bands have 40. In addition, two bands, 13 and 14, have such high SNR requirements that dual ten-element arrays are used for each band. Each along-scan pixel is viewed successively by an element of the two arrays, and the outputs are summed; this is called time delay and integration. Therefore, MODIS has a total of 490 detector elements. Each along-track element is called a channel, and each spectral band consists of 10, 20, or 40 channels.

The VIS and NIR FPA's utilize p-i-n photovoltaic silicon diodes. The SWIR, MWIR, and LWIR bands have photovoltaic HgCdTe detectors, except for the bands above 10  $\mu\text{m}$  (the last six), which use photoconductive HgCdTe.

### C. Electronics

The MODIS electronics perform numerous tasks, including amplification and conversion of detector outputs to 12-bit words, data formatting, command execution, control of twelve mechanisms, including the scan mirror, telemetry formatting, timing, focal plane temperature control, and power conditioning and distribution. These functions are performed via two analog modules (boxes) and a main electronics module (MEM) using a total of 47 printed wiring boards.

The analog modules provide all clocks and biases to the focal planes, condition the analog signals from the detectors, and convert the outputs to 12-bit words. All other functions are performed in the MEM.

The digital outputs from the analog modules are input to a format processor in the MEM, consisting of a single board computer. There is a requirement that the output from all 36 bands when viewing a given pixel be output in a single Consultative Committee for Space Data Systems (CCSDS) packet. A second requirement is that, since the focal planes when imaged on the earth are as long as 30 km (i.e., 30 consecutive sampling periods or frames), the processor must remove the temporal delays, generate the packets, and store them in a FIFO buffer prior to transmission to the spacecraft. A second identical computer in the MEM provides telemetry and command processing. Both computers are redundant and fully programmable from the ground.

### D. Onboard Calibration

The MODIS design includes four onboard calibration modules, including a solar diffuser (SD), solar diffuser stability monitor (SDSM), spectral radiometric calibration assembly (SRCA), and blackbody (BB) (see Figs. 1 and 2). In addition, there are plans to fully utilize prelaunch calibration and characterization data and postlaunch vicarious calibration data, including data from airborne sensors, buoys, ships, and globally distributed field sites.

1) *Solar Diffuser*: The SD, a pressed plate of polytetrafluoroethylene, is located behind a deployable door on the forward or along-track wall of the MODIS. The diffuser fills the entrance aperture and is viewed each scan line. However, SD readings are essentially zero except when the door is open and the sun is in view. In order for all of the 20 reflected solar

bands to be on scale during solar calibration, a second level is required. This is achieved by means of a deployable, 8.5% transmission screen located at the door aperture.

2) *Solar Diffuser Stability Monitor*: The SD enables on-orbit monitoring of system radiometric response. Response changes can arise either from the MODIS degradation or a change in the bidirectional reflectance distribution function (BRDF) of the diffuser. Therefore, the SD reflectance must be independently monitored. This is the task of the SDSM. The SDSM is basically a 5-cm diameter integrating sphere with nine spectral filter and silicon detector pairs on its inner wall and an optomechanical front end that enables the system to successively view the illuminated SD, a dark region, and the sun. The solar view has a fixed 2% transmitting screen to insure that the SD and solar levels are similar. The solar aperture for the SDSM and the opening for the SD are covered by the same door. Outputs are used to form ratios of the SD and solar views that are directly traceable to spectral reflectance of the SD.

3) *Spectral Radiometric Calibration Assembly*: The SRCA is a complex assembly used to monitor on-orbit spectral, spatial, and radiometric performance. The device includes a source assembly, a spectrometer and an output collimator. The source assembly includes an integrating sphere with four lamps (1–1 W and 3–10 W), order sorting and neutral density filters, and a thermal source. The spectrometer has an interchangeable grating and mirror and several slit and reticule combinations. The collimator directs the spectrometer output to the scan mirror and fills approximately one-quarter of the MODIS aperture. With the grating in place, the monochromatic output of the system can be stepped through the VIS, NIR, and SWIR bandpasses to measure system spectral response. With the mirror replacing the grating and along- and cross-track reticules placed alternately at the exit port of the spectrometer and with both the integrating sphere and the thermal source operating, both along-track and cross-track band-to-band registration can be measured for all bands. Finally, with the mirror in place of the grating and both the entrance and exit aperture wide open, the integrating sphere can be used as a multilevel radiometric source to monitor the MODIS radiometric response in the VIS, NIR, and SWIR bands.

4) *Blackbody*: The full-aperture onboard BB is a V-groove design with 45° included angle that has been black anodized to give an effective emissivity of >0.992. The BB provides dc restoration (a known radiance level; zero for reflected solar bands and BB temperature for thermal bands). In addition to the BB, the scan mirror views space each scan line, thereby enabling a two-point radiometric calibration of the 16 thermal bands every 1.477 s. Ordinarily, the BB floats at the MODIS operational temperature, but the temperature can be commanded and controlled to as high as 315 K. BB temperature measurements are made via 12 evenly spaced precision thermistors.

## IV. INSTRUMENT PERFORMANCE

A comprehensive testing program was executed on the MODIS Protoflight Model (PFM), the sensor scheduled to fly

on the EOS-AM1 spacecraft in 1998. These tests had two purposes. The first was to demonstrate compliance with the NASA performance specifications. The second, and perhaps more important purpose, was to supply the extensive characterization data needed to convert the digital output from the MODIS to geometrically located calibrated radiance. A description of the algorithms for this conversion is given by Guenther *et al.* [18]. The tests included characterization of the instrument's physical and performance parameters, including spatial, spectral, radiometric, and stray light response. The testing program acquired in excess of 300 GB of data from the PFM, not all of which have been processed. The summary below is the best estimate at this time of the instrument performance. Updates may be made as more information and improved algorithms are developed. Only summary information is provided here; more details are available in the SBRS test report documentation and from the MODIS Calibration Support Team (MCST) at the MCST homepage (<http://www.gsfc.nasa.gov/MODIS/MCST/Home.html>).

### A. Physical Characteristics

#### (Size, Mass, Power, and Data Rate)

Completion of the MODIS PFM has allowed accurate measurements of the instrument's physical properties, including size, mass power, and data rate. Provided here are summary values for reference only. The overall instrument size is  $1.044 \times 1.184 \times 1.638$  m, not including sunshade protrusions and open nadir and space view doors. The instrument mass was determined by direct measurement to be 228.73 kg (504.25 lbs). Orbital average power with the onboard BB in the heated condition and the MODIS in full science mode is 162.5 W. The data rate of the MODIS is 10.6 Mbps during day mode and 3.1 Mbps during night mode.

### B. Spatial Performance

As described above, the MODIS has three nominal GIFOV's at nadir: 250, 500, and 1000 m. Measurements made at the system level allow accurate characterization of the instrument spatial response profile or line spread function (LSF). Fig. 3 shows data obtained by imaging the projection of a slit in the scan and track directions across the MODIS field of view for band 10, channel 6. The resulting LSF's are representative of all bands in the MODIS, with most bands having slightly more image blur. Also shown in Fig. 3 is a small amount of optical crosstalk found in bands 33–36 (band 35, the worst case, is shown). The crosstalk was traced to a gap in the detector substrate where light can enter. The problem has been corrected in the second instrument (Flight Model 1).

The full width at half maximum (FWHM) values for the center channels in the bands are shown in Table III. We see that there is some variation of the as-built spatial resolutions as a result of the manufacturing and assembly processes. Table III also gives the scan and track centroid position of each of the bands of the MODIS relative to the average for all bands. These values were obtained in thermal vacuum from the SRCA. These numbers may change slightly (<50 m) in

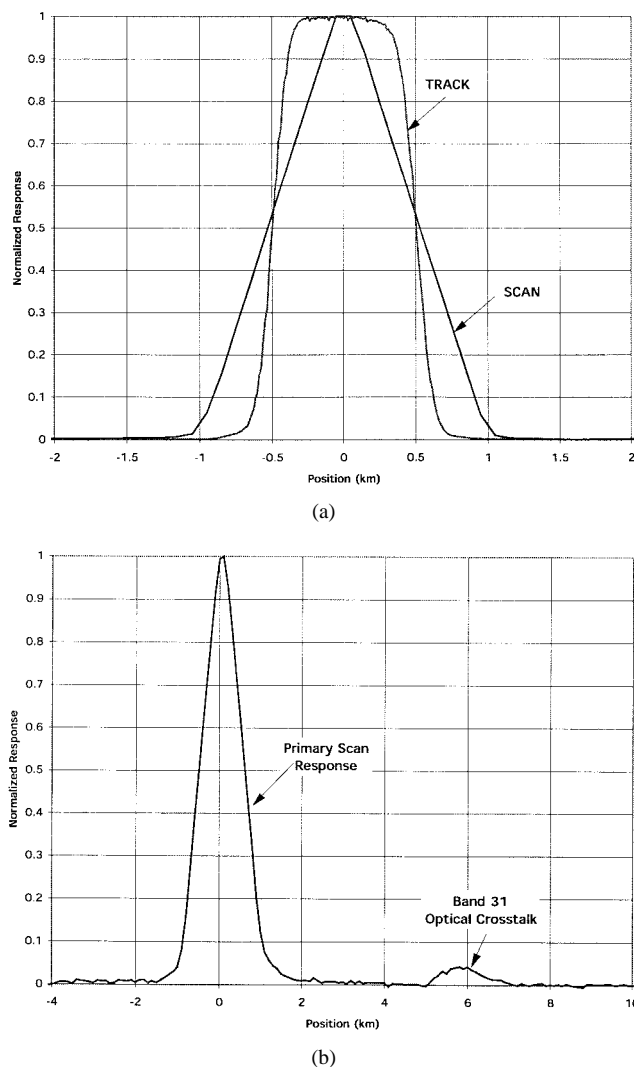


Fig. 3. Typical LSF's for MODIS. (a) Band 10, channel 6. Scan-direction LSF's are triangular due to the integration blur of the pixels in the scanning direction. Track-direction LSF's are more rectangular. (b) Band 35 has a  $\approx 5\%$  leak in the region of band 31 in the scan direction.

orbit, but these changes can be tracked with the SRCA through an on-orbit measurement of the band-to-band registration.

The LSF's for the MODIS are transformed to provide the modulation transfer function (MTF). MTF's for the MODIS at the Nyquist frequency [ $1/(2 \times \text{nominal spatial resolution})$ ] are also given in Table III.

### C. Spectral Performance

Relative spectral response (RSR) profiles were acquired in two different environments. Bands 29–36 were acquired in a clean room and bands 1–28 during thermal vacuum testing. A calcium fluoride ( $\text{CaF}_2$ ) window on the thermal vacuum chamber prevents transmissions of wavelengths beyond  $8 \mu\text{m}$  without significant absorption. The RSR's for all spectral bands are shown in Figs. 4–6.

For bands 1–28, the MODIS was in the thermal vacuum chamber while the test monochromator, the spectral measurement assembly (SpMA), was external to the chamber in a purged nitrogen environment. It is estimated that the low water

TABLE III  
PFM PIXEL SIZE, BAND-TO-BAND REGISTRATION, AND MTF

Band	Scan Size* (m)	Track Size* (m)	Scan Pos. † (m)	Track Pos. † (m)	Scan MTF (@Nyquist)	Track MTF (@Nyquist)
1	299.6	261.5	6.1	25.8	0.37	0.42
2	291.1	253.9	12.6	22.5	0.41	0.45
3	560.0	499.1	2.4	-21.3	0.38	0.54
4	546.1	499.3	-15.9	-37.2	0.40	0.56
5	540 (est.)	520 (est.)	-20.4	-65.9	0.26	0.50 (est.)
6	540 (est.)	520 (est.)	10.2	-30.4	0.27	0.50
7	537.8	521.3	-28.3	-23.8	0.34	0.46
8	1059.4	1007.4	-5.4	-28.7	0.38	0.59
9	1043.0	1002.8	7.4	-10.2	0.40	0.60
10	1058.0	1002.8	31.1	-2.2	0.40	0.60
11	1041.1	990.7	-35.0	-46.7	0.41	0.60
12	1053.5	984.1	-71.5	-60.1	0.40	0.60
13	1037.6	1000.7	6.3	18.6	0.40	0.60
14	1043.0	1009.4	-46.3	51.2	0.40	0.60
15	1042.4	1004.3	-34.6	50.2	0.41	0.60
16	1045.4	1007.2	-43.0	46.3	0.41	0.60
17	1049.3	1016.9	-54.8	47.9	0.40	0.60
18	1019.4	1001.5	16.3	4.7	0.41	0.60
19	1027.4	997.6	37.6	8.7	0.41	0.60
20	1027.4	997.6	39.4	-74.0	0.34	0.51
21	1081.3	1002.6	14.8	-91.4	0.38	0.57
22	1081.3	1002.6	57.0	-55.5	0.34	0.51
23	1035.9	1006.5	25.4	-57.2	0.40	0.55
24	1056.9	1012.6	2.4	-64.4	0.40	0.57
25	1042.0	1010.0	-11.7	-40.6	0.40	0.59
26	1060.9	1012.4	-30.8	-25.0	0.40	0.58
27	1110.3	1012.8	80.5	49.7	0.36	0.58
28	1091.0	1015.8	67.0	34.6	0.36	0.56
29	1122.3	1021.5	26.2	-18.9	0.35	0.57
30	1102.8	1005.5	95.5	39.9	0.36	0.59
31	1120.0	1012.5	-31.5	30.9	0.34	0.54
32	1078.3	1012.0	-128.0	30.6	0.37	0.55
33	1126.0	1004.3	-17.3	71.6	0.34	0.55
34	1131.5	989.8	-24.0	78.3	0.33	0.53
35	1137.8	997.3	-10.5	70.9	0.33	0.49
36	1128.3	1011.3	71.0	71.1	0.34	0.48

(est.) Bands estimated based on similar band performance. No measured data available

\* Scan and Track Sizes are measured at FWHM of the measured LSF's and have not been corrected for slit size

† Scan and Track Positions are relative to band-averaged position of all bands. Values subject to small change at launch

absorption, critical for bands 26 and 27, was achieved and the residual water vapor had negligible impact on the measured spectral response of these bands. It should be noted that band 8 has considerable polarization-dependent spectral behavior within the band that may cause uncertainty in the as-measured RSR. (See polarization discussion below).

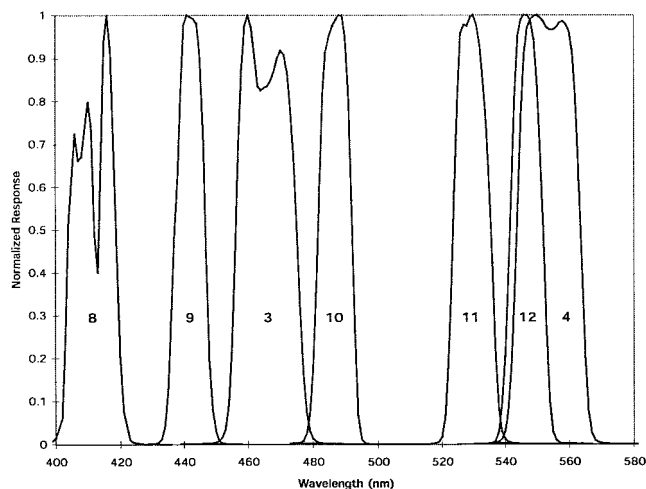
Bands 29–36 were measured in the ambient environment. Atmospheric absorption correction is small in these bands, but not insignificant, particularly for band 35. A first-order correction was applied to the data for bands 31–36 only. The latter are subject to revision via additional calibration analyses of the SpMA and application of updated atmospheric transmission data.

Table IV provides a subset of the measured RSR performance parameters for all MODIS bands. Requirements exist for each of the MODIS bands to meet the needs of the scientific community. All noncompliances are identified in the table with an “H” or an “L” to indicate the value is “High” or “Low,” relative to specifications defined by NASA. Also provided in the table is the band “centroid,” which is a spectrally weighted integration of the RSR function, where center wavelength (CW) is defined as the midpoint between

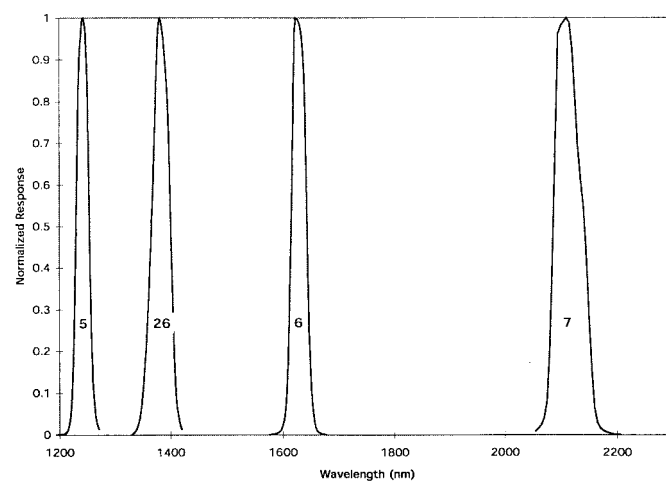
the 50% response points. Bandwidth (BW) is defined as the wavelength range between the 50% response points, and Edge Ranges (ER1 is shorter of the CW, ER2 is greater than the CW) are defined as the wavelength range between the 80% and 20% response points. The MODIS out-of-band response was characterized using broadband filters as well as scanning the double monochromator across the out-of-band spectral region over which each detector responds. The out-of-band response is defined as the ratio of the integrated response outside the 1% of peak response points (upper and lower) to the integrated response inside the 1% response points. The data are not fully processed due to the large amount acquired. However, preliminary results show excellent out-of-band rejection with no major anomalies other than the band 31 leak described above. These data are anticipated to demonstrate out-of-band instrument response of less than 0.1%.

#### D. Radiometric Performance

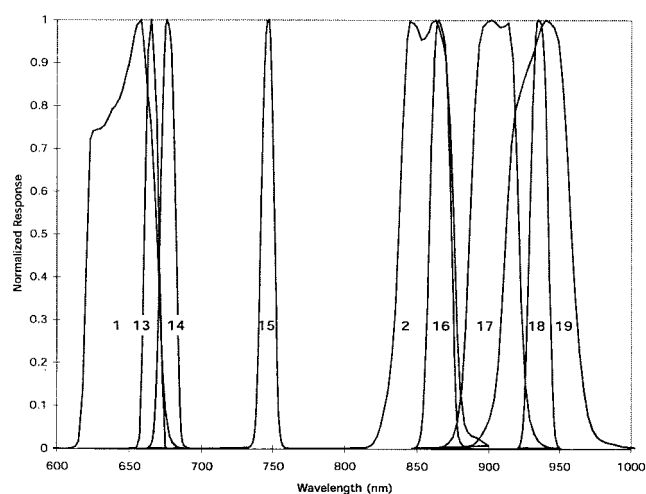
1) *Sensitivity (SNR and NEDT)*: The MODIS radiometric sensitivity was measured as SNR's and/or noise equivalent differences in temperature (NEDT's) during thermal vacuum



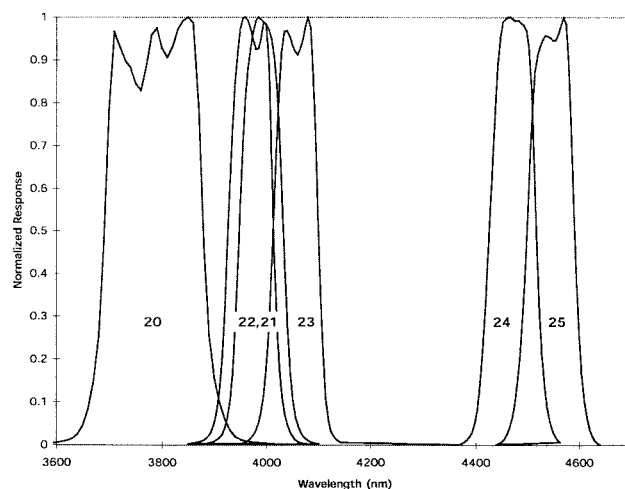
(a)



(a)



(b)



(b)

Fig. 4. (a) VIS Relative Spectral Response (RSR) profiles. (b) NIR RSR profiles. Data acquired at system level during thermal vacuum testing at nominal instrument temperature.

Fig. 5. (a) SWIR RSR profiles. (b) MWIR RSR profiles. Data acquired at system level during thermal vacuum testing at nominal instrument temperature.

testing. Data presented here are from the “hot” plateau in the thermal cycle with the instrument optics at about 283 K. (Note that the optics is designed to run cooler than the ambient temperature to reduce thermal background emission effects.) Reflective band results are shown in Fig. 7. A 100-cm diameter spherical integrating source (SIS) was placed outside the vacuum chamber with the MODIS viewing the SIS through a fused silica port. Within the chamber in the space view port was a space view source (SVS) at near-liquid-nitrogen temperatures. Eighty scans of data were obtained, and the standard deviation of the SIS signal minus the space view signal was calculated. This result was corrected for sample-to-sample offsets for the sub-1-km bands and the resulting SNR calculated. The results shown in Fig. 5 show all bands meeting specifications, except band 7 and two channels in band 8. The overall performance is close to modeled predictions based on measurements of the critical parameters from the piecepart optical elements, focal planes, and electronics.

Fig. 8 shows the NEDT's for the MODIS emissive bands. A blackbody calibration source (BCS) was placed in the vacuum

chamber near the beginning of the earth scan sector. Again, 80 scans of data were collected and the BCS signal minus space view signal was determined. Results meet requirements for most bands, except band 35, channel 8 and band 36.

SNR and NEDT results shown in Figs. 7 and 8 are also tabulated in Table V and compared to the required SNR. Radiance levels (and temperatures) at which these measurements were made are listed in Table II(a) and (b). The reflected solar radiances in Table II(a) are “typical” for the science product listed and a SZA (solar zenith angle) of 70°.

2) *Dynamic Range*: Each of the MODIS bands has a unique maximum radiance. The full-scale signal  $L_{sat}$  of each of the MODIS bands was measured during thermal vacuum testing and is shown in Table V as a fraction of the maximum radiance specified  $L_{max}$ . Bands 3, 8, 12, 21, 31, and 32 required extrapolation since the source did not achieve high enough radiance to validate the saturation levels. The only real concern is for band 21, whose data are preliminary. For this band, the BCS could only achieve about 3.5% of full scale and data evaluation is not complete.

TABLE IV  
MEASURED PARAMETERS FROM MODIS RELATIVE SPECTRAL RESPONSE PROFILES

Band	Channel	CW (nm)	BW (nm)		ER1 (nm)	ER2 (nm)	Centroid (nm)
8	5	411.3	14.8	H	12.9	4.3	411.7
9	5	442.0	9.7		4.8	4.0	441.9
3	10	465.6	18.8		4.3	5.7	465.5
10	5	486.9	10.6		4.4	3.2	486.8
11	5	529.6	12.0	H	4.2	5.0	529.6
12	5	546.8	10.3		4.6	4.4	546.7
4	10	553.6	19.8		4.8	4.6	553.5
1	20	645.0	48.0	H	24.4	13.5	646.1
13	5	665.5	10.1		4.9	H 5.8	665.6
14	5	L 676.8	11.3	H	5.8	5.5	676.7
15	5	746.4	9.9	H	5.7	H 5.4	746.3
2	20	856.5	38.4		16.1	12.1	856.1
16	5	866.2	15.5		7.5	6.8	866.0
17	5	904.0	35.0		13.2	12.4	904.0
18	5	935.5	13.6	H	6.8	6.5	935.4
19	5	L 935.2	46.1		21.7	19.4	935.9
5	10	1241.6	24.0	H	13.8	H 13.4	1241.7
26	5	1383.0	35.0	H	27.3	H 19.1	1381.7
6	10	L 1629.1	28.6	H	14.6	H 16.1	1628.9
7	10	L 2114.1	55.7		20.5	H 36.6	2114.1
20	5	H 3785.0	187.7		49.8	54.2	3786.7
21	5	H 3990.0	H 84.4		37.3	37.1	3990.2
22	5	3970.1	H 87.6		38.5	31.8	3970.1
23	5	4056.4	H 86.7		38.9	29.1	4055.6
24	5	4471.7	91.7		40.1	35.3	4471.7
25	5	H 4545.2	92.0		43.4	34.8	4544.9
27	5	H 6752.4	L 248.1	H	175.5	II 172.8	6757.3
28	5	7333.8	327.5		150.4	145.7	7330.1
29	5	8517.9	346.0	II	201.2	135.8	N/A
30	5	9736.7	301.4	H	185.7	II 193.5	N/A
31	5	11017.2	536.7		192.6	255.9	11015.7
32	5	12032.4	524.6		108.2	140.5	12025.1
33	5	13358.8	310.3		109.5	126.0	13356.2
34	5	13674.5	326.9		118.3	130.5	13674.6
35	5	13907.0	333.4		115.6	122.4	13906.4
36	5	14191.5	289.8		130.6	H 227.2	14189.7

Finally, in this table, is the measured dynamic range  $L_{\text{sat}}/\text{NEDL}$ . Dynamic ranges in excess of 7000 are sometimes required to achieve the high signal levels for bright scenes without saturation while also maintaining low noise over dark targets. Unique focal plane technology for MODIS makes this possible by employing high quantum efficiency detector materials and low noise readout amplifiers optimized for each channel.

3) *Linearity*: The MODIS linearity was characterized during thermal vacuum testing of the instrument's radiometric response. The radiometric sources (SIS and BCS) were transitioned to several radiance levels and MODIS data acquired. The resulting instrument response was then fit to a second-order polynomial to obtain the instrument response profile. The nonlinearity, shown in Fig. 9, is defined here as the ratio of the second-order term  $\times \text{DN} (@L_{\text{typ}})$  divided by the first-order term  $(a_2 \times \text{DN} (@L_{\text{typ}})/a_1)$ , where DN is the digital response of the system and  $\text{DN} (@L_{\text{typ}})$  is the response at the typical radiances listed in Table II.

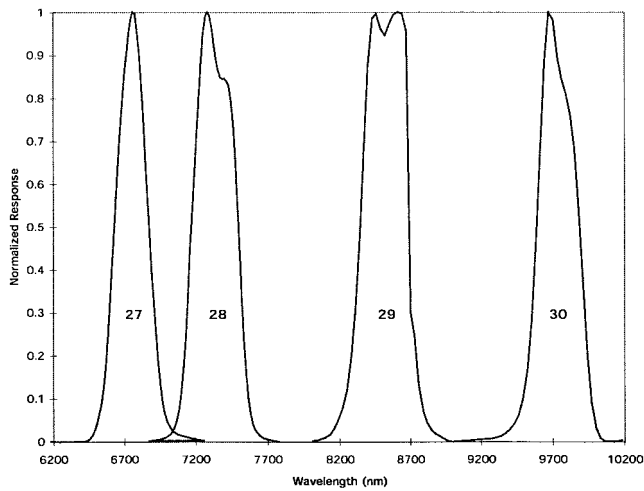
### E. Polarization

The MODIS requires less than 2% polarization sensitivity for wavelengths from 0.43 to 2.2  $\mu\text{m}$  between scan angles of  $\pm 45^\circ$ . Polarization sensitivity ( $P$ ) is defined as

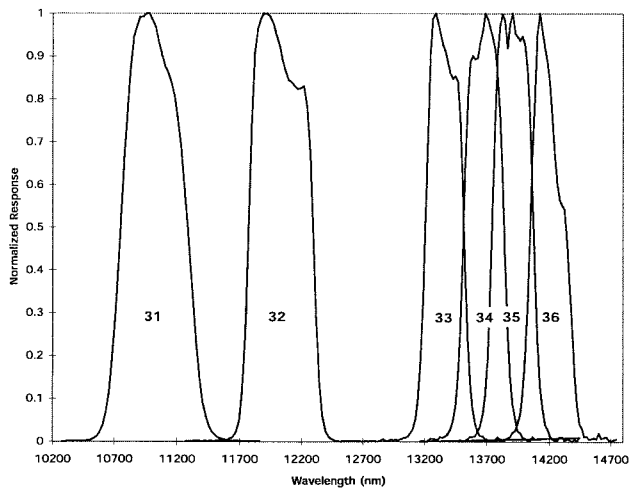
$P = (I_{\text{max}} - I_{\text{min}})/(I_{\text{max}} + I_{\text{min}})$ , where  $I_{\text{max}}$  and  $I_{\text{min}}$  are the maximum and minimum responses of the MODIS to a linearly polarized source. Band 8 is below 0.43  $\mu\text{m}$  and was not included in the specification. A polarized source assembly (PSA) provides full-aperture polarized energy to the MODIS. The polarized energy is rotated through 0–360° and a polarization response is measured. Fourier filtering of the resulting response is performed to remove any test equipment modulation. Fig. 10 gives the measured and predicted polarization factor for all measured reflective bands at scan angles of  $\pm 45^\circ$ ,  $\pm 22.5^\circ$ , and  $0^\circ$ . Bands 2 and 5 were not measured, and modeled data are not available for the SWIR bands 5–7 and 26. Performance is compliant for most bands at most scan angles. Noncompliances have been examined by members of the MODIS Science Team responsible for atmospheric corrections over oceans and were found to have only minor impact on the resulting oceanic-derived products. Table VI provides the polarization factor in tabular form for all reflective bands at all measured scan angles.

### F. Response Versus Scan Angle

During subsystem level testing, it became evident that the MODIS scan mirror with its protective-coated silver surfaces has a reflectance that is a function of both wavelength and



(a)



(b)

Fig. 6. (a) LWIR photovoltaic detector (PV) band RSR profiles. Bands 27 and 28 were acquired in thermal vacuum. Bands 29 and 30 were acquired in ambient. (b) LWIR photoconductive detector (PC) band RSR profiles were acquired in ambient. All data were acquired at system level.

angle of incidence (AOI). The latter results in a system-level change of response with scan angle. The radiometric accuracy requirements (errors <5% in the solar reflected bands and <1% in the thermal emitted bands) mandate a knowledge of the system-level response versus scan angle to approximately 0.5% for the reflected solar bands and 0.1% for the emitted thermal bands. Tests were performed in ambient by rotating the MODIS about the scan mirror rotation axis with the spherical integrating source and the blackbody calibration source in the scan plane. The reflected solar bands were found to have a change in reflectance that varied <2% over AOI's from 10.5 to 65.5° ( $\pm 55^\circ$  scan), with corresponding thermal band changes of up to 10%. The latter values, however, did not achieve the required accuracy due to instabilities in the test apparatus. Therefore, the MODIS team has requested a postlaunch maneuver of the EOS-AM1 spacecraft that will enable a full scan ( $\pm 55^\circ$ ) of space. Modeling indicates that the signal from the warm optics will be sufficient to characterize the thermal band response versus

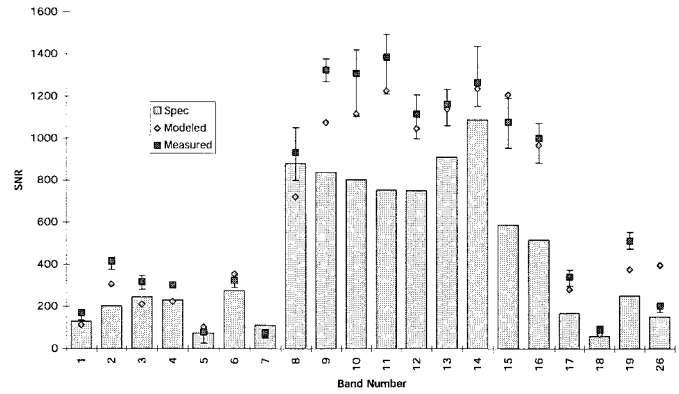


Fig. 7. SNR's for MODIS reflective bands. Error bars represent channel dependencies within a band. Radiances are for an SZA of 70°.

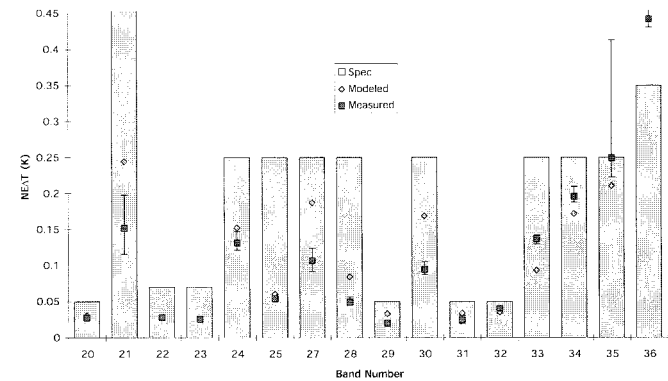


Fig. 8. NEAT's for MODIS emissive bands. The band 21 requirement is 2.0 K. Band 35, channel 8 has more noise than the other channels in the band.

scan angle. Present plans call for a continuous-pitch maneuver of the spacecraft approximately 60 days after launch.

G. Stray Light

Stray light rejection in the MODIS has two parts: near-field response (NFR) and far-field response (FFR). NFR is defined as scattered light within about  $\pm 30$  km ( $\pm 2.44^\circ$ ) of the peak response. FFR is defined as the region from roughly  $\pm 2^\circ$  to the end of scan at  $\pm 55^\circ$ .

1) *Near-Field Response:* The MODIS NFR requirements are quite stringent, calling for the reflected solar bands to settle to within 0.5% of their final value within two 1-km pixels after scanning off a bright cloud onto an ocean scene.

A scatter measurement assembly (ScMA) was used to measure the instrument NFR. This device consists of a high-energy tungsten filament source for the reflective bands and a ceramic source for the infrared bands at the focus of a single 30-cm diameter low-scatter spherical mirror. The source image is scanned by the MODIS to produce an instrument response profile. The peak signal is saturated, but the near-field region has sufficient SNR to measure better than  $10^{-6}$  of peak instrument response for the reflective bands and  $10^{-4}$  for the emissive bands.

The near-field data are then normalized to provide a total instrument response, as shown in Fig. 11. This response for band 12, channel 5 is typical of the data observed in the

TABLE V  
SNR, NEDL, AND NEDT MEASURED AT THE RADIANCES (AND TEMPERATURES GIVEN IN TABLE II(a) AND (b)) AND THE FRACTION OF FULL-SCALE RADIANCE ACHIEVED AND THE DYNAMIC RANGE

Band	SNR	SNR	NEDL	NEDT	Lsat/Lmax*	Lsat/NEDL
	Measured	Required	(W/m <sup>2</sup> -sr- $\mu$ m) Measured	(K) Measured	Measured	Measured
1	168.1	128.0	0.1304	-	1.11	5837
2	413.5	201.0	0.0598	-	0.97	4638
3	315.7	243.0	0.1120	-	1.19	6285
4	302.2	228.0	0.0960	-	1.13	6122
5	77.6	74.0	0.0750	-	1.19	1747
6	324.1	275.0	0.0226	-	1.07	3312
7	72.0	110.0	0.0143	-	1.14	1753
8	932.8	880.0	0.0484	-	1.28	4627
9	1324.6	838.0	0.0317	-	1.15	4845
10	1307.9	802.0	0.0247	-	1.14	4675
11	1385.0	754.0	0.0183	-	1.12	5003
12	1114.3	750.0	0.0189	-	1.12	3806
13	1162.6	910.0	0.0082	-	1.14	4466
14	1264.7	1087.0	0.0069	-	1.14	5108
15	1076.6	586.0	0.0095	-	1.12	3045
16	1000.0	516.0	0.0062	-	1.14	4654
17	339.5	167.0	0.0296	-	1.00	6232
18	89.9	57.0	0.0404	-	1.12	7088
19	510.0	250.0	0.0295	-	1.12	7184
20	882.4	470.2	0.0005	0.0275	1.06	3564
21	203.2	158.7	0.0117	0.1519	0.69(TBR)	5031
22	893.3	352.6	0.0008	0.0277	1.06	2680
23	975.3	364.1	0.0008	0.0255	1.07	2863
24	146.6	78.0	0.0012	0.1313	7.63	2236
25	440.3	95.2	0.0013	0.0540	3.11	2044
26	201.0	150.0	0.0300	-	1.09	3254
27	254.4	107.4	0.0046	0.1063	3.52	2480
28	648.8	126.7	0.0034	0.0490	2.74	3639
29	2698.6	1065.6	0.0036	0.0197	1.12	4577
30	446.2	168.5	0.0083	0.0945	2.81	2154
31	2792.4	1362.3	0.0034	0.0244	1.06	9050
32	1839.5	1475.2	0.0049	0.0402	0.99	5127
33	451.1	247.0	0.0100	0.1367	1.82	1192
34	299.1	233.5	0.0126	0.1955	2.27	908
35	220.1	220.6	0.0141	0.2492	2.47	774
36	106.9	135.1	0.0195	0.4418	4.09	621

TBR - To Be Reviewed

\* Sub-km bands averaged over even/odd samples to 1-km effective size

MODIS NFR measurements. It should be noted that within two pixels of the peak, the MODIS response is down to one part in 1000, and it is falling rapidly. The figure shows two collects of the data, showing extremely good repeatability down to  $10^{-6}$  in response. Features responsible for the instrument response profile are clearly seen, including the primary detector response, ghosting, the intermediate field stop, and scan mirror scatter. Table VII provides the radiometric error of a pixel at radiance  $L_{typ}$  located 2 km from the edge of a bright cloud (or  $L_{max}$  for emissive bands) of size 10 km in track  $\times$  20 km in scan. This result is obtained by integrating the NFR for each band (similar to that shown for band 12 in Fig. 11) and normalizing by the ratio of  $L_{cloud}$  (or  $L_{max}$ )/ $L_{typ}$ . The integration is performed for scan angles less than the peak (NFR\_NEG) and greater than the peak (NFR\_POS). The requirement of 0.5%  $L_{typ}$  is not achieved for most bands.

2) *Far-Field Scattered Light*: A special far-field scattered light test was performed using the ScMA. This test produced instrument response profiles from  $10^{-6}$  to  $10^{-8}$  of peak response, but did not achieve the full range of angles due

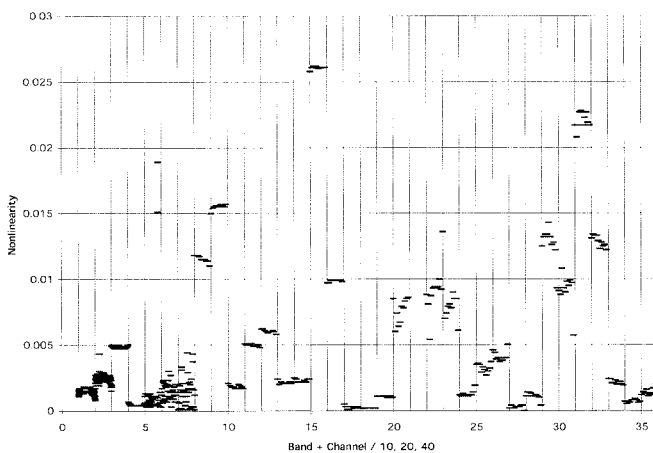


Fig. 9. MODIS nonlinearity. MODIS bands show high linearity for most bands. Calibration coefficients are being developed to minimize the impact to system calibration of any nonlinear response.

to SNR constraints. Another test using a solar simulator was performed to test the overall image quality degradation when scanning a bright target out to  $\pm 55^\circ$ . This test demonstrated

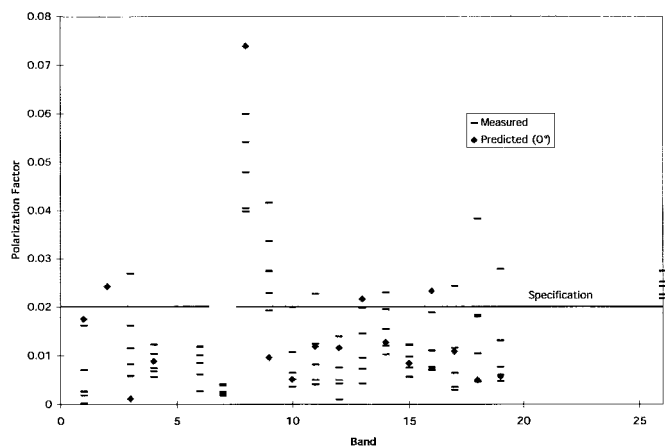


Fig. 10. MODIS polarization for reflective bands for measured scan angles of  $\pm 45^\circ$ ,  $\pm 22.5^\circ$ , and  $0^\circ$ . There is a “best effort” requirement on band 8. No measured data is available for bands 2 and 5, and no data exists for the SWIR bands 5–7 and 26.

TABLE VI  
MEASURED POLARIZATION FACTORS FOR THE MODIS REFLECTIVE BANDS

Band	Scan Angle $-45^\circ$	Measured Scan Angle $-22.5^\circ$	Polarization Scan Angle $0^\circ$	Factor Scan Angle $22.5^\circ$	Scan Angle $45^\circ$
1	0.016	0.003	0.002	0.000	0.007
2	N/A	N/A	N/A	N/A	N/A
3	0.006	0.008	0.012	0.016	0.027
4	0.010	0.007	0.007	0.006	0.012
5	N/A	N/A	N/A	N/A	N/A
6	0.012	0.003	0.008	0.010	0.006
7	0.004	0.002	0.003	0.002	0.004
8	0.040	0.040	0.048	0.054	0.060
9	0.019	0.023	0.027	0.034	0.042
10	0.006	0.004	0.005	0.011	0.020
11	0.004	0.005	0.008	0.012	0.023
12	0.008	0.004	0.001	0.005	0.014
13	0.004	0.007	0.010	0.015	0.020
14	0.010	0.012	0.016	0.020	0.023
15	0.006	0.008	0.010	0.012	0.012
16	0.007	0.007	0.008	0.011	0.019
17	0.003	0.003	0.006	0.012	0.024
18	0.010	0.005	0.018	0.018	0.038
19	0.006	0.008	0.005	0.013	0.028
26	0.027	0.024	0.025	0.023	0.022

NA - Not Available

good image saturation recovery with virtually no overshoot and no far-field ringing or memory effects.

V. SUMMARY AND CONCLUSIONS

Testing of the MODIS PFM instrument is complete; critical physical attributes and performance characteristics have been determined. The instrument size, mass, power, and data rate are all within specification limits. Spatial performance test results provide the instrument ground footprint characteristics and MTF values at Nyquist for all bands. The instrument spectral response has been characterized in thermal vacuum (for bands sensitive to atmospheric absorption) and ambient (for bands whose wavelengths do not transmit through the chamber window). The RSR profiles and critical spectral performance parameters have been provided. Instrument ra-

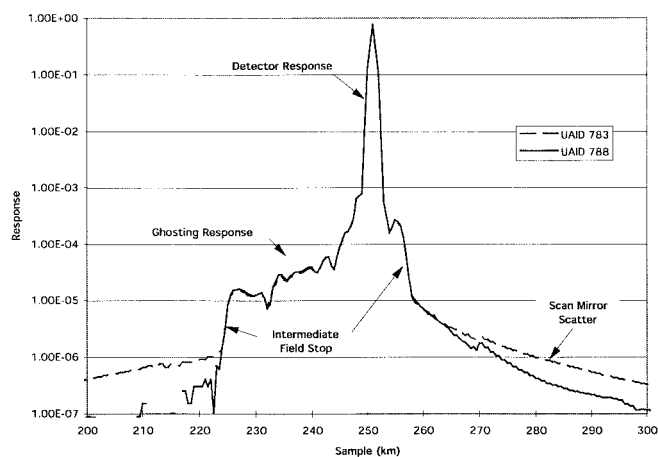


Fig. 11. Measured near-field response for band 12, channel 5. Two measurements show a high degree of repeatability down to  $1E-6$ . The figure also shows contributors to features shown.

TABLE VII  
INTEGRATED NFR (RADIOMETRIC ERROR) AS A PERCENTAGE OF  $L_{typ}$  FROM A CLOUD 20 km IN SCAN  $\times$  10 km IN TRACK LOCATED 2 km FROM A REGION OF  $L_{typ}$

Reflective Band	NFR_NEG (%Ltyp)	NFR_POS (%Ltyp)	Emissive Band	NFR_NEG (%Ltyp)	NFR_POS (%Ltyp)
1	1.00	0.82	20	5.87	6.91
2	3.20	2.89	21	5.87	6.91
3	1.60	1.55	22	9.65	0.55
4	2.01	1.63	23	5.49	0.03
5	N/A	N/A	24	0.02	4.24
6	N/A	N/A	25	0.01	3.06
7	1.12	5.10	26	1.06	3.27
8	1.89	2.61	27	0.87	0.35
9	1.70	2.19	28	1.58	2.13
10	1.55	2.09	29	0.30	1.25
11	1.64	1.34	30	0.06	0.46
12	2.36	1.51	31	1.39	0.09
13	7.16	6.19	32	2.27	0.46
14	7.65	7.44	33	2.09	1.31
15	3.70	5.09	34	3.16	1.75
16	3.62	4.74	35	3.18	1.55
17	1.50	2.56	36	N/A	N/A
18	7.40	4.95			
19	1.58	0.60			

NA - Not Available

diometric sensitivity (SNR and NEDT) and dynamic range show excellent performance meeting (and in many cases, exceeding) the majority of requirements. Many of the reflected solar bands demonstrate SNR's that exceed 1000:1 for a solar zenith angle of  $70^\circ$ . The instrument linearity has been characterized and calibration algorithms are being developed to include the effects of minor nonlinearities. MODIS meets the polarization requirements for most bands and scan angles. All noncompliances were reported to the MODIS Science Team, and values were deemed low enough and algorithms flexible enough to meet all science objectives. Instrument NFR has been well characterized, but it fails to meet the stringent worst-case specifications. This has implications on radiometric accuracy near high-contrast edges, and correction algorithms that utilize the extensive test data are being pursued.

The MODIS FFR shows no ringing, memory effect, or other artifacts and demonstrates excellent saturation recovery.

The MODIS has been delivered to and integrated on the EOS-AM1 spacecraft. Extensive system-level tests are ongoing, and launch is scheduled for 1998.

#### ACKNOWLEDGMENT

The design, manufacture, calibration, and characterization of the MODIS have been truly monumental tasks lasting over 14 years. During this period, several hundred talented professionals have dedicated themselves to creating a system that all believe will be a major contribution to earth remote sensing. Of special note are R. Weber, MODIS Instrument Manager, EOS-AM1 Project, GSFC, L. Tessmer, MODIS Project Manager, SBRS, and J. Young, Systems Engineer, SBRS.

#### REFERENCES

- [1] M. D. King, D. D. Herring, and D. J. Diner, "The earth observing system (EOS): A space-based program for assessing mankind's impact on the global environment," *Opt. Photon. News*, vol. 6, no. 34, p. 39, 1995.
- [2] V. V. Salomonson, W. L. Barnes, P. W. Maymon, H. E. Montgomery, and H. Ostrow, "MODIS: Advanced facility instrument for studies of the Earth as a system," *IEEE Trans. Geosci. Remote Sensing*, vol. 27, pp. 145–153, Mar. 1989.
- [3] W. E. Esaias and W. L. Barnes, "Moderate Resolution Imaging Spectrometer (MODIS) instrument panel report," *Earth Observing Syst. Rep.*, NASA, 1986, vol. Iib, 59 pp.
- [4] OAO Corporation, "MODIS definition study," NASA, OAO Corp., Greenbelt, MD, Contract NAS 5-27157 modification no. 5, Final Rep., 1985.
- [5] ITT Aerospace, "Phase-A study report on the MODIS-N spectrometer for the earth observing system," ITT Aerospace/Optical Div., Fort Wayne, IN, 1985.
- [6] T. J. Magner and V. V. Salomonson, "Moderate resolution imaging spectrometer-tilt (MODIS-T)," *Int. J. Imaging Syst. Technol.*, vol. 3, pp. 121–130, 1991.
- [7] S. W. Running, C. O. Justice, V. V. Salomonson, D. Hall, J. Barker, Y. J. Kaufman, A. Strahler, A. R. Huete, J.-P. Muller, V. Vanderbilt, Z. Wan, P. Teillet, and D. Carneggie, "Terrestrial remote sensing, science and algorithms planned for EOS/MODIS," *Int. J. Remote Sensing*, vol. 15, no. 17, pp. 3587–3620, 1994.
- [8] M. D. King, Y. J. Kaufman, W. P. Menzel, and D. Tanré, "Remote sensing of cloud, aerosol, and water vapor properties from the Moderate Resolution Imaging Spectrometer (MODIS)," *IEEE Trans. Geosci. Remote Sensing*, vol. 30, pp. 2–27, Jan. 1992.
- [9] V. V. Salomonson and D. L. Toll, "Execution phase (C/D) spectral band characteristics of the EOS Moderate Resolution Imaging Spectrometer-NADIR (MODIS-N) Facility Instrument," *Adv. Space Res.*, vol. 11, no. 3, pp. 231–236, 1991.
- [10] H. R. Gordon, "Radiometric considerations for ocean color remote sensors," *Appl. Opt.*, vol. 29, pp. 3228–3236, 1990.
- [11] H. R. Gordon and A. Y. Morel, *Remote Assessment of Ocean Color for Interpretation of Satellite Visible Imagery: A Review*. New York: Springer-Verlag, 1983, p. 114.
- [12] J. J. Susskind, J. Rosenfield, D. Reuter, and M. T. Chahine, "Remote sensing of weather and climate parameters from HIRS-AMSU on TIROS-N," *J. Geophys. Res.*, vol. 89D, pp. 4677–4699, 1984.
- [13] Y. J. Kaufman and B. C. Gao, "Remote sensing of water vapor in the near IR from EOS/MODIS," *IEEE Trans. Geosci. Remote Sensing*, vol. 30, pp. 871–884, Sept. 1992.
- [14] B. C. Gao and A. F. H. Goetz, "Column atmospheric water vapor retrievals from airborne imaging spectrometer data," *J. Geophys. Res.*, vol. 95, pp. 3549–3564, 1990.
- [15] B. C. Gao and Y. J. Kaufman, "Selection of the 1.375  $\mu\text{m}$  MODIS channel for remote sensing of cirrus clouds and stratospheric aerosols from space," *J. Atmos. Sci.*, vol. 52, pp. 4231–4237, 1996.
- [16] B. C. Gao, A. F. H. Goetz, and W. J. Wiscombe, "Cirrus cloud detection from airborne imaging spectrometer data using the 1.38 micron water vapor band," *Geophys. Res. Lett.*, vol. 20, no. 4, pp. 301–304, 1993.
- [17] Goddard Space Flight Center, "Specification for the Moderate Resolution Imaging Spectroradiometer (MODIS)," Greenbelt, MD, 422-20-22, 1993.
- [18] B. Guenther, G. D. Godden, X. Xiong, E. J. Knight, S.-Y. Qiu, H. Montgomery, M. M. Hopkins, M. G. Khayat, and Z. Hao, "Prelaunch algorithm and data format for the Level 1 calibration products for the EOS-AM1 Moderate Resolution Imaging Spectroradiometer (MODIS)," this issue, pp. 1142–1151.



**William L. Barnes** received the B.S. and M.S. degrees in physics from North Texas State University, Denton, and the Ph.D. degree in physics from Florida State University, Tallahassee.

He was a member of the Professional Staff of the Southwest Research Institute, San Antonio, TX, for four years and has held a variety of positions in science, engineering, and management at NASA's Goddard Space Flight Center, Greenbelt, MD, over the past 27 years. He is presently the Associate Chief of the Laboratory for Hydrospheric Processes, a Member of the MODIS Science Team, and has been contributing toward the development of MODIS for over 14 years.



**Thomas S. Pagano** received the B.S. degree in physics from the University of California at Santa Barbara in 1982 and the M.S. degree in physics from Montana State University, Bozeman, in 1984.

He was with Raytheon Santa Barbara Remote Sensing, Goleta, CA, for 12 years, has received two United States patents, and has authored numerous technical papers on space remote-sensing systems. He was the Chief Systems Engineer on the MODIS PFM from conceptual design through the build, test, and spacecraft integration. He is currently with the Jet Propulsion Laboratory, California Institute of Technology, Pasadena. His specialty is in systems performance analysis and modeling.

**Vincent V. Salomonson** (SM'92–F'98), for a photograph and biography, see this issue, p. 1041.